

Reactive oxygen species (ROS) dependent antibacterial effects of graphene oxide coatings

C. Zhao ^{a,d,*}, L. Zhang ^b, H. Wu ^c, X. Song ^d, Y. Chen ^c, D. Liu ^d, P. Lei ^d, L. Li ^d, B. Cui ^a

^a*School of Medicine, Hubei Polytechnic University, Huangshi 435003, China.*

^b*Department of Pharmacy, Changhai Hospital, Naval Medical University, Shanghai 200433, China.*

^c*School of Public Health, Xinxiang Medical University, Xinxiang, Henan, 453003, China.*

^d*School of Life Sciences and Technology, Xinxiang Medical University, Xinxiang, Henan, 453003, China.*

The antibacterial mechanism of GO in solution have been well studied, however, the antibacterial activity of GO as coating material in solid phase is still unclear. Here, we report a direct proof of the antibacterial mechanisms of GO coatings. Oxidative stress induced by GO coating was found to be an important reason for the prevention of bacteria colonization on the coating surface, since a ROS dependent antibacterial effect was detected in this study. This finding could help with understanding bacteria-GO solid surface interaction and further designing such antibacterial implant surfaces.

(Received April 2, 2021; Accepted April 7, 2022)

Keywords: Reactive oxygen species, Graphene oxide, Antibacterial activity

1. Introduction

Since it was reported to show antibacterial effects against a broad spectrum of bacteria [1-4], GO has attracted considerable attention worldwide for its great potential application in antibacterial coating materials. According to the previous reports, the antimicrobial activity of GO was influenced by its quality, size, forms and other factors[5, 6]. So far, there are three main GO antibacterial activities, are reported. 1. The first mechanism is called nano-knife model which means that the sharp edges of GO sheets can physically cut the bacterial membrane and led to the leakage of cytoplasmic constituent and death of the microorganism[7]; 2. The second mode of antibacterial action is associated with oxidative stress induced by charge transfer and a reactive oxygen species (ROS)[8, 9]; 3. Microorganisms can be wrapped and isolated from the surrounding environment and dead due to the lack of nutrition[10].

* Corresponding author: 15921061530@163.com

<https://doi.org/10.15251/DJNB.2022.172.481>

The antibacterial mechanism of GO solid coating can be quite different from GO in solution, however, only few studies reported the antibacterial activities, and the exact mechanism is still not clear.

In this study, since the coating is solid and flat, the wrapping mechanism can be ignored, and nano-knife action has weakened a lot, we suppose that the oxidative stress effect is the main antibacterial activity. Therefore, we concentrate our attention to the amounts of GO for preparing the coatings. The samples preparation strategy was shown in Figure S1. Three GO coatings with different amounts of GO were fabricated by spin coating, the activities of *Escherichia coli* (*E. coli*, ATCC 25922) on GO coatings were investigated. Furthermore, The ROS generated after *E. coli* and GO interaction was detected.

2. Experimental section

2.1. Preparation of GO coatings on SiO₂ substrates

Aqueous GO suspension (10 g·L⁻¹; Graphene Supermarket) was diluted with deionized (DI) water to 7mg mL⁻¹, 4 mg mL⁻¹, 1 mg mL⁻¹ respectively. SiO₂ substrates (diameter 14 mm, thickness 1 mm) were washed by ultrasonication in acetone, methanol, and anhydrous ethanol for 10 min respectively, followed by rinsing with DI water for 10 min. The samples were degreased by sonication in acetone, methanol, and ethyl alcohol, and drying at 100 °C for 30 min. After drying at 80 °C for 1 hour in an air oven, the samples were immersed in 2% (3-aminopropyl) triethoxysilane (APTES, Sigma-Aldrich) ethanol solution (5 mL) for 40 min to obtain aminosilane-functionalized discs. Then the samples were left to dry again at 80 °C for 1 hour in nitrogen atmosphere. Finally, GO coatings were self-assembled on the aminosilane-functionalized SiO₂ substrates by spin coating. Briefly, GO water dispersing solution (1 mg mL⁻¹, 4 mg mL⁻¹, 7mg mL⁻¹) was dropped on the surface of SiO₂ substrate respectively, and the substrate was spin coated at 100 rpm for 5 s, and at 2000 rpm for 30 s to obtain the 3 different GO coatings on the surface, named GO-1, GO-4, GO-7 respectively.

2.2. Characterization

The morphology and size of GO sheets were detected by atom force microscopy (AFM, Bruker Dimension 3100); the surface morphology of GO coating was characterized by Scanning Electron Microscope (SEM, Zeiss Supra 60 VP); the surface elemental composition of GO coating was characterized by Energy Dispersive Spectrometer (EDS, EDAX EDS Elite T).

2.3. Antibacterial activity evaluation

The antibacterial performance of GO coating was evaluated by *Escherichia coli* (*E. coli*, ATCC25922) using a procedure adapted from previous publications[11, 12]. The coating samples were sterilized in 70 % ethanol aqueous solution, then bacterial cell suspension (10⁷ CFU mL⁻¹) was introduced onto the coated surface to a density of 60 μL cm⁻². After 24 h of incubation, the dissociated bacterial solution was immediately spread on LB agar media and cultured overnight at 37 °C. Colony counting method was employed to analyze the viability of *E.coli* after interaction with GO coating.

Bacterial cell viability can be calculated by formula (1):

$$\text{Bacterial Cell Viability (\%)} = \frac{N_{\text{Experiment}}}{N_{\text{Control}}} \times 100\% \quad (1)$$

$N_{\text{Experiment}}$: The number of bacteria in the experimental group (CFU mL⁻¹).

N_{Control} : The number of bacteria in the control group (CFU mL⁻¹).

In addition, a Live/Dead fluorescent staining assay was performed to show the cell viability on the sample. Cell suspension at a concentration of 10⁷ CFU mL⁻¹ was inoculated on the sample to a density of 60 μL cm⁻². After incubation overnight, the culture medium was removed and the samples were rinsed with physiological saline, stained by using a the LIVE/DEAD BacLight™ Bacterial Viability Kit (L13152, Molecular Probes) was used to stain in the dark for 20 min and then observed with the fluorescent microscope (Nikon 80i).

2.4. Assay of ROS

The intracellular level of ROS was directly displayed by ROS fluorescence staining. Briefly, 10⁷ CFU mL⁻¹ bacterial suspensions were inoculated on the sample surfaces at a density of 60 μL cm⁻². After culture overnight, the culture medium was removed and the samples were rinse in PBS, stained by a ROS Asay Kit (Shanghai beyotime Biotechnology Co., Ltd) for 20min, then rinsed with stroke-physiological saline solution and observed under a fluorescence microscope(Nikon 80i).

2.5. Statistical Analysis

Antibacterial studies were performed in quadruplicates for each group. The values were expressed as mean ± standard deviation. The statistical analysis was performed using the Student's T-test and $p < 0.05$ or 0.01 in the differences between groups was considered to be significant or extremely significant.

3. Results and discussion

3.1. Characterization of GO and GO coatings

Graphene oxide nanosheets were purchased from Graphene Supermarket in this study. The obtained aqueous GO suspension was diluted to obtain a GO solution with a concentration of 50 μg mL⁻¹ for AMF analysis. The results showed that GO nanosheets were mostly monolayer and bilayer with irregular shape, height around 1 nm and lateral sizes of ~200–250 nm (Figure S2).

The morphology of GO-1, GO-4, GO-7 and the SiO₂ surface were investigated by SEM. As shown in Fig. 1, the pristine SiO₂ has a flat and clear surface, while all GO coatings with wrinkles was clearly seen particularly for GO-4 and GO-7 samples. EDS results (Figure 2) showed that C content increased in the order of GO-1, GO-4, and GO-7 (~5%, 7%, and 9% respectively), indicating the amount of GO increased in the same order.

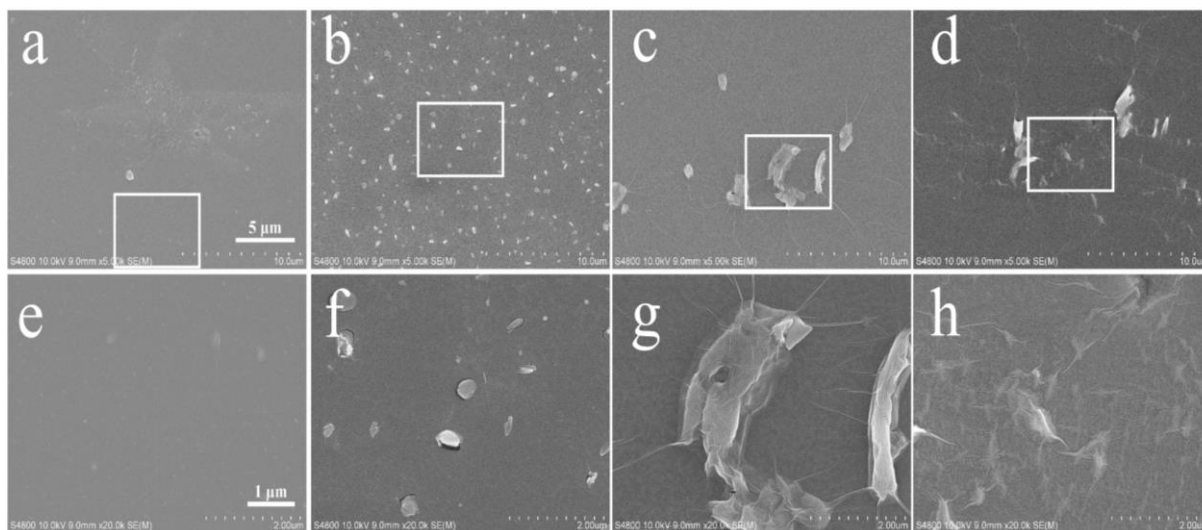


Fig. 1. SEM images of SiO₂ substrate(a and e, scale bar 5 μm, 1 μm respectively,);GO-1 coating (b and f, scale bar 5 μm, 1 μm respectively); GO-4 coating (c and g, scale bar 5 μm, 1 μm respectively);and GO-7 coating (d and h, scale bar 5 μm, 1 μm respectively).

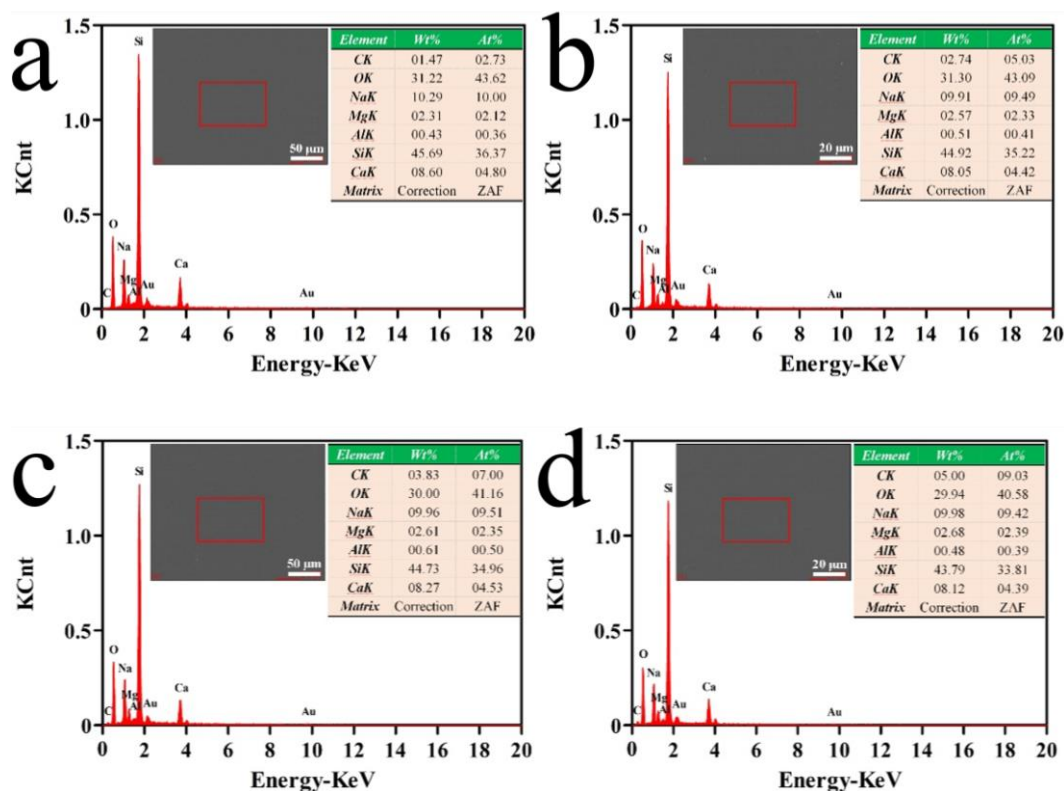


Fig. 2. EDS mappings of the SiO₂ substrate(a), GO-1 coating(b), GO-4 coating(c), and GO-4 coating(d).

3.2. Antibacterial Activity of GO coatings

Figure 3 showed the typical pictures and colony forming units counting results of *E. coli* after incubation with GO coating samples. A large number of bacterial colonies can be seen on the agar medium for the control group, which indicated that *E. coli* can survive well on the SiO₂ substrate. The number of colonies was decreased in the order of GO-1, GO-4, and GO-7. Particularly for GO-7 group, no bacterial colonies were found, which means that *E. coli* cell growth was inhibited completely after incubation with GO-7. Cell viability of *E. coli* was calculated and shown in Figure 3b. Compared with SiO₂ control, significant loss of viability was found on GO-1 (lost 40%), GO-4 (lost 75%), and GO-7 (lost 100%) surfaces.

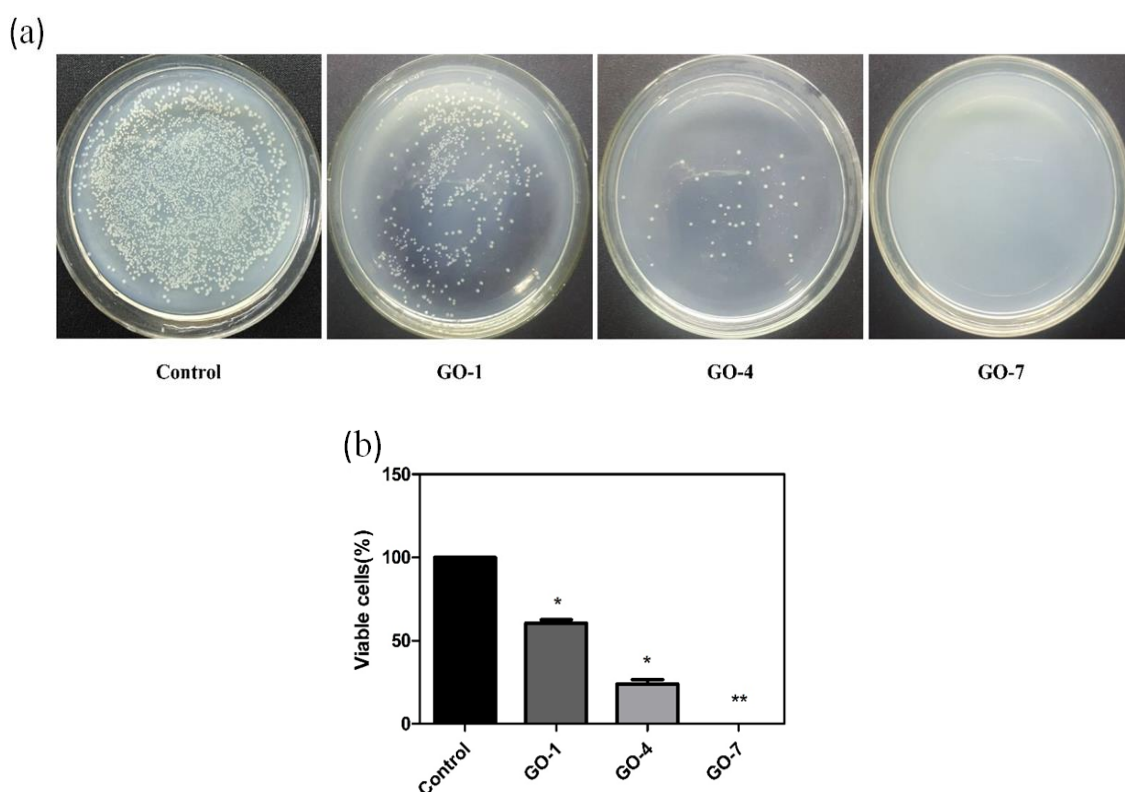


Fig. 3. *E. coli* cell response to GO coatings. (a) Typical photographs of re-cultivated *E. coli* colonies on agar culture plates, with the seeded concentrations of 10^7 CFU/ml; (b) Cell viability measurement by CFU counting after incubation with various coatings and re-culture on agar culture plates, * $p < 0.05$, ** $p < 0.01$ compared with control.

Live/Dead fluorescent staining was further used to visualize the survival status of *E. coli* on respective surfaces. The representative fluorescent images are presented in Figure 4. After culture overnight, most viable *E. coli* cells (green) were observed on the control surface while the amounts of viable cells were evidently lower and the dead cells (red) increased dramatically on the GO coating surfaces. Particularly, GO-7 surface showed the highest intensity in red, suggesting that the number of dead cells were the highest in all groups. Both GO-4 and GO-7 surfaces showed excellent antibacterial activities confirmed by large amounts of dead cells. And GO-1 showed

relatively lower antibacterial activities, this trend is consistent with the CFU counting result described above.

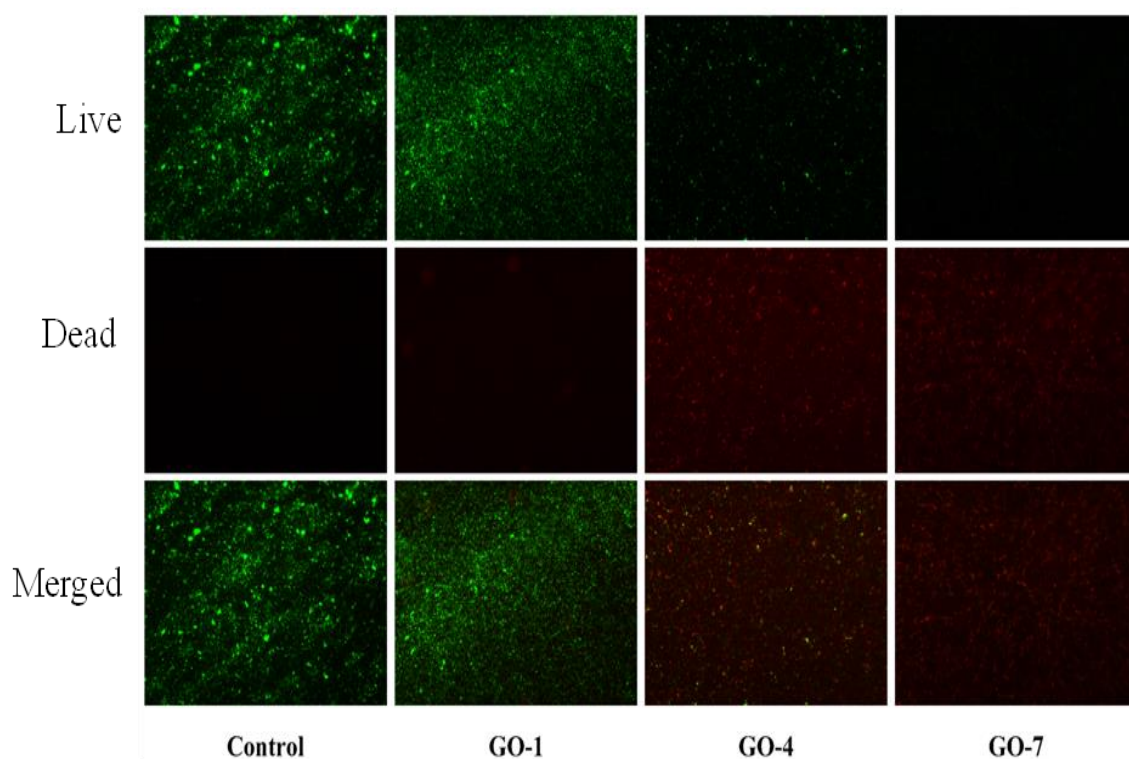


Fig. 4. Live/dead fluorescent staining images of *E. coli* on GO coatings.

3.3. Generation of intracellular ROS

ROS are a series of crucial signaling molecules in oxidative stress response, including $\cdot\text{O}_2^-$, H_2O_2 , $\cdot\text{OH}$, etc., which are generated by the successive single-electron reductions of molecular oxygen [13]. A small amount of intracellular ROS generation can promote cell growth[14], while the excessive production of ROS can cause oxidative stress[13, 15], and induce oxidative damage, which eventually leads to mitochondrial dysfunction and cell death. As shown in Figure 4, compared with the control group, the fluorescence intensities in GO-1, GO-4, and GO-7 groups were increased significantly after *E. coli* incubation with GO coating samples, and the fluorescence intensities increased in the order of GO-1, GO-4, and GO-7, suggesting that the generation of ROS increased in the same order. It demonstrated that after interaction with GO coatings, the intracellular ROS generation was significantly enhanced, particularly in GO-7 group which showed the highest ROS level.

3.4 Proposed mechanism for the ROS dependent antibacterial activity of GO coatings

As we described above, there are three main antibacterial activities of GO nanomaterials according to the previous publications. However, the wrapping mechanism is not likely to happen, since in the solid coating GO sheets cannot move around, and the bacterial cells would attached on the coating rather than wrapped by the coating. Therefore, the rest two mechanisms (Physical

contact destruction and Oxidative stress antibacterial) could be important for the GO coatings.

The alignment of graphene oxide nanosheets was reported to influence the antibacterial activities by regulating the physical contact way between bacteria cells and GO nanosheets[5]. The vertical GO film was found to enhance the antibacterial activities than the random film and the planar one. In their study, phospholipid vesicles were utilized to mimic GO–cell interactions. Their results found that membrane damage in the GO/lipid vesicle system is mainly caused by physical disruption rather than chemical mechanisms like ROS induced oxidative stress. Other similar studies also confirmed that the vertical GO coatings significantly enhanced the antibacterial activity by exposing more edges of GO sheets to bacterial cells[6, 16-18]. Overall, Physical contact destruction caused by sharp edges of vertical GO film or coating were thought to be the main reason for the enhanced antibacterial effect.

However, the antibacterial performance of the random GO film and the planar one did not show significant statistical difference compared with the control group without GO[5]. In this study, GO coatings were prepared by random alignment but with different amounts of GO sheets. SEM images confirmed that no obvious vertical GO sheets were found on all GO coating surfaces (Figure 1). Compared with GO-1, GO-4 and GO-7 showed more wrinkles in some area but all samples are flat in general. As we discussed above, vertically oriented GO nanosheets are more likely to contact directly with bacteria cells in an orthogonal fashion, which was confirmed by previous modeling studies to be beneficial for penetration of the lipid bilayer[19, 20]. For random GO coatings, it is not likely to pierce the bacterial cell membrane as easy as vertical GO coating does. We suppose that chemical mechanism (Oxidative stress antibacterial mechanism) plays a key role in the antibacterial activities of random GO coatings. The ROS detecting results confirmed that the intracellular ROS generation increased as the GO amounts rise in the coatings.

A clear ROS dependent antibacterial effect of GO coatings was shown in Figure S3, with the increase of GO sheets amounts in the order of GO-1, GO-4 and GO-7, the ROS generation and oxidative stress damage of cells increased in the same order, suggesting that the cytotoxicity of GO can be regulated by controlling GO concentration in the coating. Compared with controlling the alignment of graphene oxide nanosheets, the strategy to control the GO amounts in the coating is more effective and simple.

4. Conclusion

In conclusion, GO coatings with different amounts of GO sheets were prepared via a simple spin coating technology, the cytotoxicity of GO against *E.coli* was found to be rely on the ROS generation after incubation with GO coatings. The exact cytotoxicity mechanism of GO is complex and still unclear, it is unrealistic to evaluate all the factors which could influence the toxicity of GO. In this study, we focused on the GO amounts in the coating, and found that the antibacterial activity of GO coating is heavily dependent on the ROS generation which regulated by the GO amounts in the coating. Our study not only demonstrates a ROS dependent cytotoxicity of GO coating, but also provides a simple way to design engineering GO antibacterial coatings with regulated cytotoxicity.

Acknowledgements

This work was supported by the Key Scientific Research Projects of Higher Education of Henan Province (18A430026), the Scientific and Technological Development Foundation of Henan Province (China) [Grant No. 182102310699] and the Natural Science Foundation of Henan Province (China) [Grant No. 182300410107]. The authors acknowledge the School of Public Health, Xinxiang Medical University for the use of for the use of imaging equipment and for the support from the staff. Changhong. Zhao and Li Zhang contributed equally to this work

References

- [1] H. Fallatah, M. Elhaneid, H. Ali-Boucetta, T. W. Overton, H. El Kadri, K. Gkatzionis, *Environ Sci Pollut Res Int* 26(24), 25057 (2019); <https://doi.org/10.1007/s11356-019-05688-9>
- [2] P. Kumar, P. Huo, R. Zhang, B. Liu, *Nanomaterials (Basel)* 9(5), 737 (2019); <https://doi.org/10.3390/nano9050737>
- [3] W. Hu, C. Peng, W. Luo, M. Lv, X. Li, D. Li, Q. Huang, C. Fan, *ACS Nano* 4, 4317 (2010); <https://doi.org/10.1021/nm101097v>
- [4] M. Cacaci, C. Martini, R. Torelli, F. Bugli, M. Sanguinetti, Graphene Oxide Coatings as Tools to Prevent Microbial Biofilm Formation on Medical Device, *Advances in Experimental Medicine & Biology* (2019); https://doi.org/10.1007/5584_2019_434
- [5] X. Lu, X. Feng, J. R. Werber, C. Chu, I. Zucker, J. H. Kim, C. O. Osuji, M. Elimelech, Enhanced antibacterial activity through the controlled alignment of graphene oxide nanosheets, *Proc Natl Acad Sci U S A* (2017) 201710996; <https://doi.org/10.1073/pnas.1710996114>
- [6] Z. Jia, Y. Shi, P. Xiong, W. Zhou, Y. Cheng, Y. Zheng, T. Xi, S. Wei, From Solution to Biointerface: Graphene Self-Assemblies of Varying Lateral Sizes and Surface Properties for Biofilm Control and Osteodifferentiation, *Acs Appl Mater Interfaces* (2016) acsami.6b05198; <https://doi.org/10.1021/acsami.6b05198>
- [7] V. T. H. Pham, V. K. Truong, M. D. J. Quinn, S. M. Notley, Y. Guo, V. A. Baulin, M. Al Kobaisi, R. J. Crawford, E. P. Ivanova, Graphene Induces Formation of Pores That Kill Spherical and Rod-Shaped Bacteria, *Acs Nano* (2015) 150721083558001; <https://doi.org/10.1021/acsnano.5b03368>
- [8] A. Anisha, U. Binesh, W. Shih-Chun, Z. Lizhi, C. C. Perry, H. Chih-Ching, Graphene oxide and carbon dots as broad-spectrum antimicrobial agents - A minireview, *Nanoscale Horizons* (2018) 10.1039/C8NH00174J-.
- [9] S. Gurunathan, J. Woong Han, A. Abdal Daye, V. Eppakayala, J.-h. Kim, *International Journal of Nanomedicine* 7, 5901 (2012); <https://doi.org/10.2147/IJN.S37397>
- [10] V. Palmieri, F. Bugli, M. C. Lauriola, M. Cacaci, R. Torelli, G. Ciasca, C. Conti, M. Sanguinetti, M. Papi, M. De Spirito, *Acs Biomaterials Science & Engineering* 3(4), 619 (2017); <https://doi.org/10.1021/acsbomaterials.6b00812>
- [11] C. Zhao, S. Pandit, Y. Fu, I. Mijakovic, A. Jesorka, J. Liu, *Rsc Advances* 6(44), 38124 (2016); <https://doi.org/10.1039/C6RA06026A>

- [12] J. Li, G. Wang, H. Zhu, M. Zhang, X. Zheng, Z. Di, X. Liu, X. Wang, *Scientific Reports* 4, (2014); <https://doi.org/10.1038/srep04359>
- [13] Y. Li, J. Zhao, G. Zhang, L. Zhang, S. Ding, E. Shang, X. Xia, *Water Research* 161, 251 (2019); <https://doi.org/10.1016/j.watres.2019.06.011>
- [14] Y. Zhang, G. Shen, Y. Yu, H. Zhu, *Environmental Pollution* 157(11), 3064 (2009); <https://doi.org/10.1016/j.envpol.2009.05.039>
- [15] S. Liu, T.H. Zeng, M. Hofmann, E. Burcombe, J. Wei, R. Jiang, J. Kong, Y. Chen, *ACS nano* 5(9), 6971 (2011); <https://doi.org/10.1021/nn202451x>
- [16] S. Pandit, Z. Cao, V. R. S. S. Mokkalapati, E. Celauro, A. Yurgens, M. Lovmar, F. Westerlund, J. Sun, I. Mijakovic, *Advanced Materials Interfaces*, 1701331 (2018); <https://doi.org/10.1002/admi.201701331>
- [17] S. Pandit, K. Gaska, V. R. S. S. Mokkalapati, E. Celauro, I. Mijakovic, *Small* 16(5), (2020); <https://doi.org/10.1002/sml.201904756>
- [18] F. Alimohammadi, M. S. Gh, N. H. Attanayake, A. C. Thenuwara, D. R. Strongin, *Langmuir* 34(24), (2018); <https://doi.org/10.1021/acs.langmuir.8b00262>
- [19] Y. Li, H. Yuan, D. B. Von, A. M. Creighton, R. H. Hurt, A. B. Kane, H. Gao, *Proceedings of the National Academy of Sciences of the United States of America* 110(30), 12295 (2013); <https://doi.org/10.1073/pnas.1222276110>
- [20] J. Wang, Y. Wei, X. Shi, H. Gao, *Rsc Advances* 3(36), 15776 (2013); <https://doi.org/10.1039/c3ra40392k>